The Influence of Temeperature on the Body Doping Concentration In A Symmetric Double Gate Nano MOSFET In Quasi-Ballistic Electron Transport

[1]Sulaiman Muhammad Gana, [2]Garba Shehu Musa Galadanci, [3]Tijjani Hassan Darma, [4]Abdussalam Mubarak, [5]Abdulrazak Tijjani

[1,2,3,5]Physics Department, Bayero University Kano, P.M.B 3011, Kano State, Nigeria
[4]Department of Electrical/Electronics, Federal College of Education (Technical) Bichi, Kano, State, Nigeria,

ABSTRACT: **This paper presents the impact of body doping concentration on the electron transport in a DG-MOSFET using the quasi-ballistic (Semi-classical) model. Numerical simulations of the electronics characteristics such as the average electron velocity, drain current, electron density and sub-band energy profile are analyzed under a range of low, average and high temperatures (50K, 350K and 850K) using NanoMOS 2D device simulator. The result showed that at a lower doping concentration of $\mathbf{1E+04cm^{-2}}, \mathbf{1E+08cm^{-2}}, \mathbf{1E+12cm^{-2}}$ *and* $\mathbf{1E+16cm^{-2}}$ when the temperature increase above 50K the average electron velocity increases as the channel region between the source and the drain decreases. It was observed that the threshold voltage is more sensitive to doping concentration greater than $\mathbf{N_d = 1E+18cm^{-2}}$ and also more sensitive to the mobility of the electron at high temperature as such the average electron velocity of the doping concentration $\mathbf{N_d = 1E+19cm^{-2}}$ is relatively constant as the channel length increases above 14nm with an average electron velocity of $\mathbf{4.66E+05m/s}$. The body doping concentration increase the height of the barrier potential (electron density decrease) at all temperatures and the number of electron entering the channel decreases, this causes a decrease in the On-State current as observed from the average electron velocity. The change in the gate voltage makes the electron inversion stronger when the doping concentration increases resulting in a stronger On-State current. This shows that increases in the doping level of concentration increase the potential profile thereby decreasing the leakage current and increases in the threshold voltage.**

Index terms: **Double Gate Nano-MOSFET, Doping Concentration, Electron velocity, Electron Density, Sub-Band Energy.**

I. Introduction

Over the previous few decades, the reduction in size of MOSFET dimensions from the micrometer to the nanoscale region has surpassed bulk MOSFET technology in terms of high circuit density and performance enhancement [1, 2]. The International Technology Roadmap for Semiconductors (ITRS) precisely describes the projection and estimation of scaling the dimension of the transistor to drive the pace of semiconductor technology, particularly with respect to the Metal Oxide Semiconductor Field Effect Transistor (MOSFET) [3, 4]. A MOSFET device's gate length entered the deep submicron/nano zone in 2006, with the unique property that as they become smaller, they also become cheaper, consume less power, become faster, and enable more functionalities per unit area [5, 6, 3]. The symmetric and asymmetric double gate (DG) MOSFET unlike the bulk MOSFETs has received great attention in recent years because its architecture has two gates which provide an enhanced gate-to-channel coupling capacitance thereby reducing the short channel effect (SCE); the symmetric DG-MOSFET with the identical work function in both gates and a single input voltage supplied to both gates [7, 8, 9, 10]. In the absence of deletion charges, the DG MOSFET with an undoped body can boost carrier mobility, which contributes significantly to an effective electric field, hence reducing mobility [11, 12, 8]. To circumvent this, undoped DG MOSFETs must rely on a gate work function to achieve different threshold voltages on the chip; however, due to technical limitations, DG MOSFETs do not have a metal gate with a configurable work function. [13, 14, 12, 15]. Thus, body doping remains an alternative adjustment option for DG MOSFETS threshold voltages. [16, 12]. Huaxin et al. published a comprehensive research of the body doping effect on double-gate DG MOSFETs in 2007 and discovered that when the device is fully depleted, the threshold voltage shift owing to body doping is always proportional to the total dopant. [12]. In a 2009 study, Joseph discovered that an n-doped layer in the channel lowers the threshold voltage and increases the drive current when compared to an undoped channel device in Layer Doped Double Gate MOSFETs (LDDG MOSFETs) [17]. In 2012 a study by Vinay and Ashwani reported that changing the doping concentration changes the threshold voltage. In 2013 the effects of p-type body doping concentration on the asymmetric double-gate (DG) MOSFET using full quantum simulation to investigate the drain current, potential energy profile, 2D electron density, and on-off current ratio show that a higher body doping always improves the short channel effects [18]. There is no mention of the influence of doping concentration as temperature varies in the deep nanochannel region in the current literature. The literature focuses on the electrical properties of the devices without considering electron transport when the channel dimension is reduced to the nanoscale region. When the channel dimension is reduced to the nanoscale region, however, the classical approach fails to account for the majority of the device's behaviour and must be explained in a quantum mechanical manner. As a result, the semi-classical technique is used (classical approach governed by some quantum principle). The purpose of this study is to investigate the effect of body doping on symmetric DG MOSFETs using a semi-classical model (in which some parts of the system are treated quantum mechanically) as the physical channel length of the double-gate MOSFET is varied in 10nm increments from 0nm to 50nm, covering temperature ranges of 50K, 350K, and 850K. The influence on electron transport is studied as the source voltage is varied from 0.50V to 1.50V with a 0.10V step size along the channel to evaluate the average electron velocity, resistance, 2D electron density, and sub-band energy profile.

II. Transport Model

The Poisson equation, as well as the electron and hole continuity equations, govern carrier transport in semiconductor devices. The Poisson equation is given by [7];

$$-\nabla^2\Psi = \frac{q}{\varepsilon}(N_d - n + \mathrm{p} - N_a) + \rho_{trap} \quad (1)$$

Where **ε** is the electrical permittivity, q is the elementary electronic charge, n and p are the densities of electron and hole, N_d is the concentration of donor ion, N_a is the concentration of acceptor ion, and the charge density contributed by traps and fixed charges is ρ_{trap}. The continuity equation for the electron is given by [7]:

$$\nabla \cdot J_n = qR + q\,\frac{\partial_n}{\partial_t} \quad (2)$$

$$-\nabla \cdot J_n = qR + q\,\frac{\partial_n}{\partial_t} \quad (3)$$

The electron density at a certain energy level is defined as the product of the Local Density of State (LDOS) and Fermi distribution at that energy [19, 20].

$$\mathrm{n\,(E)} = \mathrm{D\,(E)f\,(E)} \quad (4)$$

where $n\ (E)$ is the electron density at energy E, $D\ (E)$ is the local density of state at energy $E\ and\ f\ (E)$ fermi distribution of the electron at energy E [20]. Natori's theory [21] of ballistic MOSFETs highlights the importance of the source to channel barrier [22, 23]. The threshold voltage (V_T) of a MOSFET is determined by measuring the drain current for various values of gate voltage in the linear regime (at low V_{DS} values) and the drain current in the linear region is obtained by [24, 4];

$$I_D = \frac{\mu C_{ox} W}{L}\left(V_{GS} - V_T - \frac{V_{DS}}{2}\right)V_{DS} \quad (5)$$

where V_T represents the threshold voltage, V_{GS} represents the gate to source voltage, V_{DS} represents the drain to source voltage, μ is the carrier mobility, C_{ox} represents the oxide capacitance, W represents the channel width, and L represents the channel length. The resistance R_{Load} of nano-MOSFET at the quasi-ballistic limit can be calculated by [25, 26];

$$R_{load} = \left(\frac{V_{DS}}{I_{DS}}\right) = \frac{V_{th}}{I_{on-state\ at\ linear\ region} \times W} \quad (6)$$

III. Methodology

NanoMos 4.0.0.2 is a 2-D simulator for thin body (less than 5 nm) devices that employs a Green's function method and a basic scattering treatment based on the concept of Büttiker probes [20]. The double gate device architecture allows for an efficient mode space approach, which significantly reduces the computational cost and allows it to be used as a design tool. To account for carrier transit along the channel, the transport models consider quantum effects in the confinement direction [27].

Simulation Procedure

The simulation technique runs concurrently with the transport model, which is self-consistently solved with Poisson's equation, as explained in Equation (1). The Poisson equation convergence parameter was set to be $1.0E-06\ eV$ and the self-consistency convergence parameter was set at $0.001\ eV$. The source voltage is varied from 0.50V to 1.50V with a step size of 0.10V and the top and bottom gate contact work function was fixed at $4.188\ eV$ with Aluminum gate material and the top and bottom dielectric material as silicon dioxide (SiO_2). The simulation is done by varying the doping concentration at $N_d = 1\mathrm{E}+04\ \mathrm{cm}^{-2}$, $N_d = 1\mathrm{E}+08\mathrm{cm}^{-2}$, $N_d = 1\mathrm{E}+12\mathrm{cm}^{-2}$, $N_d = 1\mathrm{E}+16\ \mathrm{cm}^{-2}$, $N_d = 1\mathrm{E}+18\ \mathrm{cm}^{-2}$ and $N_d = 1\mathrm{E}+19\mathrm{cm}^{-2}$ for different temperatures of 50k, 250k, 350k, 450k, 650k and 850k through a channel dimension of 0nm to 50nm. The channel material used is Silicon (Si) and the silicon film thickness (TSi) is set to be a constant 3nm with the Top/bottom oxide insulator thickness (TOX) of 1nm. The simulation is done using the following procedure;

- The device is modelled by selecting device type (Double gate MOSFET)
- Selecting Transport Model for the device geometry (ballistic transport using semiclassical Approach) and input bias parameters are inputted.
- Devices description parameters are selected.
- Simulation options are inputted (vertical and Horizontal Nodes spacing, convergence parameters, and Number of subbands).
- The program is run to obtain results.

The initial parameters for channel body acceptor impurity concentration (N_a) was set at 1.00E+12/$cm^3$and the Top and Bottom Relative Dielectric constant were 3.9 and the body Relative Dielectric constant was 11.7. The body doping is intrinsic and the source and drain terminals are heavily n+ doped with arsenic at $1.0E12\ cm^{-3}$ to obtain the 2D electron density along the channel describing the relationship between a certain electron density distribution and the electric field under high and low drain bias. The source and drain overlap are set to zero and temperatures are varied from 50K, 350K, and 850K for each value of the doping concentration $N_d = 1\text{E} + 04\ \text{cm}^{-2}$, $1\text{E} + 08\text{cm}^{-2}$, $1\text{E} + 12\text{cm}^{-2}$, $1\text{E} + 16\ \text{cm}^{-2}$, $1\text{E} + 18\ \text{cm}^{-2}$ and $N_d = 1\text{E} + 19\text{cm}^{-2}$ to obtain the average electron velocity in the sub-band described by the thermal velocity and the electron density at a certain energy level to obtain the sub-band energy profile along the channel.

IV. Result and Discussion

To analyze and study the effect of temperature on the doping concentration of the symmetric DG MOSFET in nanoscale ranging from L =00nm to L= 50 nm the semi-classical electron transport is employed. It was observed that the 2D average electron velocity for body doping concentration $N_d = 1\text{E} + 04\ \text{cm}^{-2}$, $N_d = 1\text{E} + 08\text{cm}^{-2}$ and $N_d = 1\text{E} + 12\text{cm}^{-2}$ at 50K of temperature showed an identical output characteristic with a higher average electron velocity of $9.22E + 05\ m/s$ at 7.5nm as seen in Fig. 1. The resistance and the gate voltage plot in Fig. 2 showed the same characteristics with a decrease in resistance as the gate voltage increases for both $N_d = 1\text{E} + 04\ \text{cm}^{-2}$, $N_d = 1\text{E} + 08\text{cm}^{-2}$ and $N_d = 1\text{E} + 12\text{cm}^{-2}$. At $N_d = 1\text{E} + 16\text{cm}^{-2}$ the average electron velocity exhibit the same behaviour with a slightly lower peak value of $9.23E + 05\ m/s$at 7.5nm, this is also seen from the resistance and the gate voltage plot in Fig. 2.

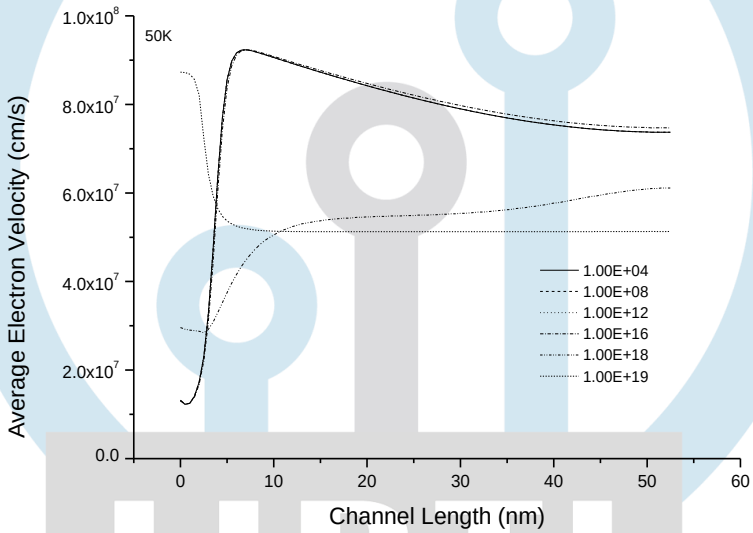

Figure 1: Average electron velocity at 50K

The doping concentration $N_d = 1\text{E} + 04\ \text{cm}^{-2}$, $N_d = 1\text{E} + 08\text{cm}^{-2}$, $N_d = 1\text{E} + 12\text{cm}^{-2}$ and $N_d = 1\text{E} + 16\text{cm}^{-2}$ the average electron velocity decreases as the channel increases from 7.5nm to 50.5nm and reached a minimum value of $7.37E + 05\ m/s$. At $N_d = 1\text{E} + 18\text{cm}^{-2}$ the average electron velocity is $2.96E + 05\ m/s$ at 0.0nm and increases as the channel length increase before it reaches a maximum value at 50.5 nm with an average electron velocity of $6.11E + 05\ m/s$. When the doping concentration is $N_d = 1\text{E} + 19\text{cm}^{-2}$ the average electron velocity is relatively constant at $5.13E + 05m/s$ throughout the channel region. This shows that the drain current is almost consta

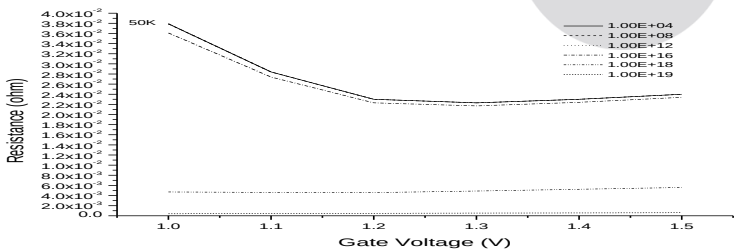

nt, with slightly constant resistance from the source to the drain throughout the channel at higher doping concentration and increases slightly with increasing channel dimension.

Figure 2: Gate Voltage vs Resistance at 50K

It was observed that at a lower doping concentration with an increase in temperature the average electron velocity increases when the channel region between the source and the drain is narrowed to break through the barrier potential, and when the channel length has widened the velocity of the electron becomes relatively constant with the increasing channel region as observed in Fig. 3 when the temperature is 350K. It is reported by Ziabari et al. in 2013 that there is a barrier potential region near the source of the channel that always determines the number and amount of electrons entering the channel from the drain [18]. The resistance is lower at 350K compared to the resistance at 50K of temperature as shown in Fig. 4. When $N_d = 1\mathrm{E} + 18\mathrm{cm}^{-2}$ the average electron velocity increases at 0.0nm and increases as the channel length increases and when $N_d = 1\mathrm{E} + 19\mathrm{cm}^{-2}$ the average electron velocity is relatively constant throughout the channel region. This shows that an increase in the doping concentration with increasing temperature increases the average electron velocity when the channel dimension is smaller and does not have much effect as the distance between the source and the drain widens. This behaviour is reported by Vinay and Ashwani in 2012 that as we decrease the channel doping the average electron velocity decrease and also increasing the channel doping increases the average electron velocity and this increases the saturation threshold voltage of the device [7].

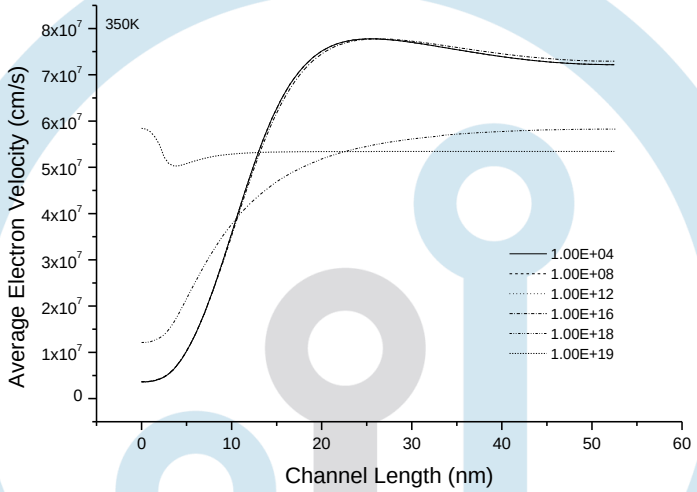

Figure 3: Average electron velocity at 350K

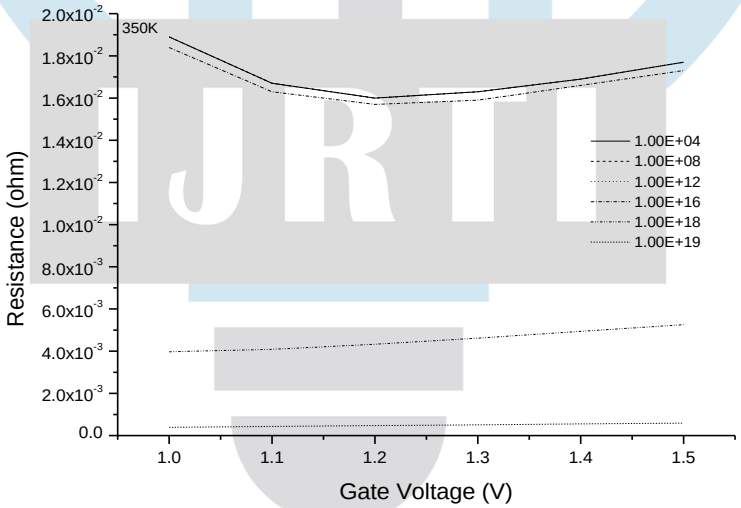

Figure 4: Gate Voltage vs Resistance at 350K

The gate voltage always increases as the channel length increases and at very high temperatures (850K) the average electron velocity also increases because the barrier potential is a bit loose and the resistance through the channel is lowered so the electron can freely drift from the source to the drain along the channel region as shown in Fig. 6.

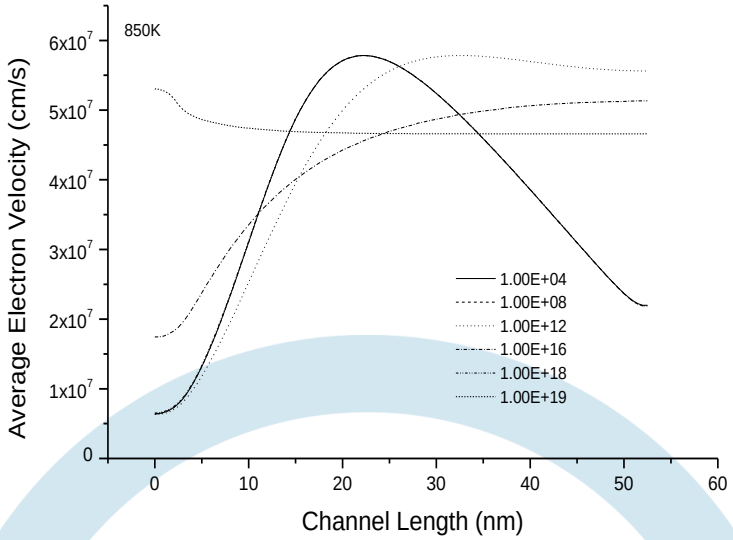

Figure 5: Average electron velocity at 850K

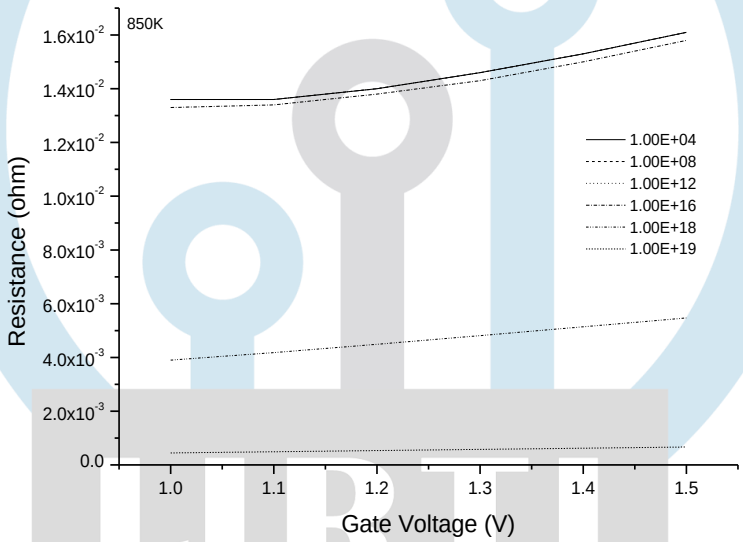

Figure 6: Gate Voltage vs Resistance at 850K

The change or increase in doping concentration is to increase the threshold voltage through the channel region, but at high temperature, the behaviour of the electrons is chaotic because the doping concentration alters the average distance (mean free path) of the electron before it is turned around by another electron. The threshold voltage is more sensitive to doping concentration greater than $N_d = 1\mathrm{E} + 18\mathrm{cm}^{-2}$ and also more sensitive to the mobility of the electron at high temperature as such the average electron velocity of the doping concentration $N_d = 1\mathrm{E} + 19\mathrm{cm}^{-2}$ is relatively constant as the channel length increases above 14nm with an average electron velocity of $4.66E + 05m/s$ as shown in Fig. 5. This is also reported by Ziabari et al in 2012 that the threshold voltage is not sensitive to channel doping when the concentration is below $1\mathrm{E} + 18\mathrm{cm}^{-2}$ due to a high threshold voltage that implies a higher voltage to switch the device on. The electron density along the channel for doping concentration of $N_d = 1\mathrm{E} + 04\ \mathrm{cm}^{-2}$, $N_d = 1\mathrm{E} + 08\mathrm{cm}^{-2}$ and $N_d = 1\mathrm{E} + 12\mathrm{cm}^{-2}$ Fig. 7 showed that at 50K of temperature the electron density is concentrated at $0.0\ nm$ with a peak value of $2.48 \times 10^{11} cm^{-2}$ and decrease rapidly with an increase in the channel length before becoming relatively constant above 4.5nm.

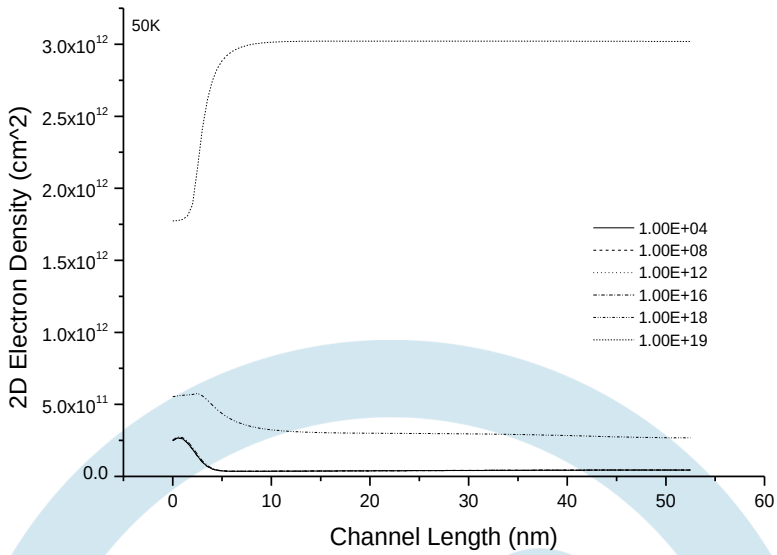

Figure 7: 2D electron Density at 50K

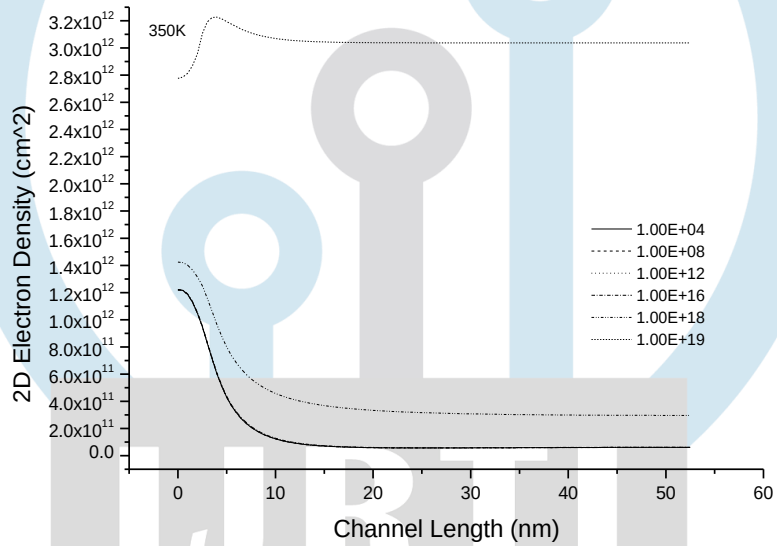

Figure 8: 2D electron Density at 350K

The electron density when the doping concentration is $N_d = 1\mathrm{E} + 16\mathrm{cm}^{-2}$ is slightly higher with a peak value of $2.54 \times 10^{11} cm^{-2}$. This is because the density of electrons at low temperature is very high to overcome the barrier potential as such the electrons are concentrated at the lowest channel region as already seen from the average electron velocity in Fig. 1. As temperature increases to 350K, and 850K as shown in Fig. 8 and Fig. 9 respectively it was observed that the doping concentration is always regulated by the height of the barrier potential in the source region as the electrons move rapidly from the source to the drain along the channel region.When the doping concentration is above $N_d = 1\mathrm{E} + 18\mathrm{cm}^{-2}$ the number of electrons increases thereby causing the source region to be populated by a large number of electrons as such high electron density is observed at all temperatures.

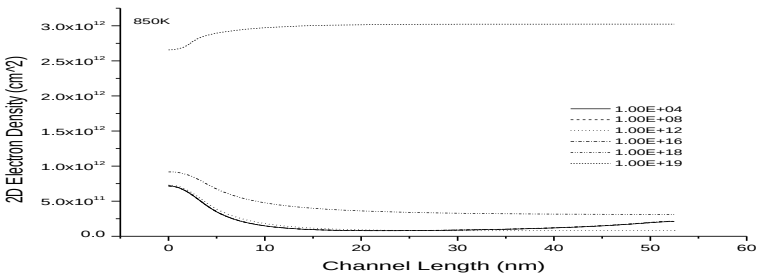

Figure 9: 2D electron Density at 850K

The barrier potential is averagely high at an average temperature this results in an averagely high electron density at 350K to be relatively constant at the lowest channel region with a peak value of $7.38 \times 10^{10} cm^{-2}$ as illustrated in Fig. 8. when the doping concentration is $N_d = 1\text{E} + 04\ \text{cm}^{-2}$, $N_d = 1\text{E} + 08\text{cm}^{-2}$ and $N_d = 1\text{E} + 12\text{cm}^{-2}$ and with a peak value of $7.52 \times 10^{10} cm^{-2}$, $2.38 \times 10^{11} cm^{-2}$ and $2.38 \times 10^{12} cm^{-2}$ when the doping concentration is $N_d = 1\text{E} + 16\ \text{cm}^{-2}$, $N_d = 1\text{E} + 18\ \text{cm}^{-2}$ and $N_d = 1\text{E} + 19\text{cm}^{-2}$ respectively.

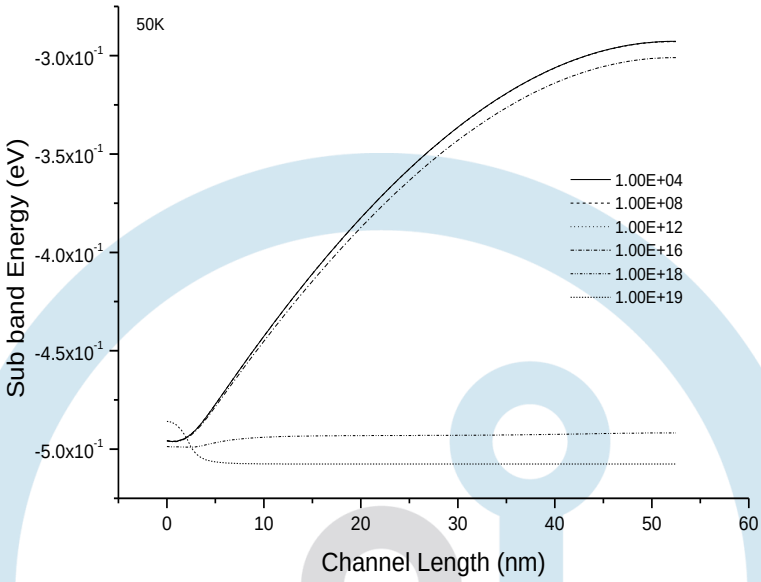

Figure 10: Sub-band energy profile at 50K

At all temperatures when the body doping concentration increase the height of the barrier potential also increases and the number of electrons entering the channel decreases this causes a decrease in the On-State current as observed from the average electron velocity in Figures 1 3, and 5. Also, as the gate voltage changes the electron inversion is stronger when the doping concentration increases resulting in a stronger On-State current.The Potential Energy of the electron (Sub-band energy) as shown in Figure 19 along the channel at Low temperature (50K) is Low with high electron density (See Figure 13) and increases as the doping concentration increase with average identical energy for $N_d = 1\text{E} + 04\ \text{cm}^{-2}$, $N_d = 1\text{E} + 08\text{cm}^{-2}$ and $N_d = 1\text{E} + 12\text{cm}^{-2}$ of $-3.76 \times 10^{-1} eV$.

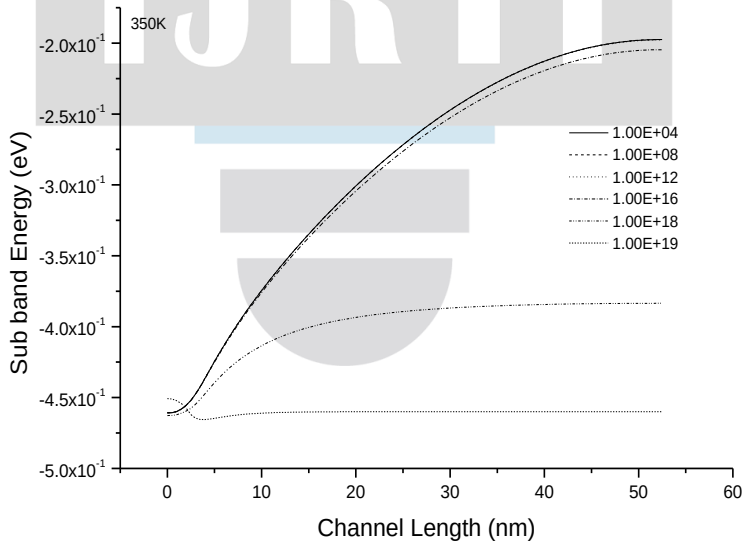

Figure 11: Sub-band energy profile at 350K

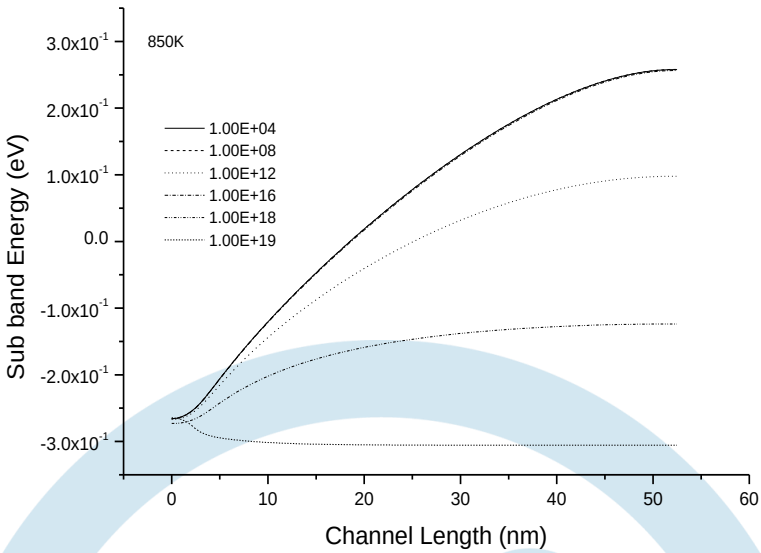

Figure 12: Sub-band energy profile at 850K

The average potential energy of the electron in the sub-band for $N_d = 1\text{E} + 16\ \text{cm}^{-2}$, $N_d = 1\text{E} + 18\ \text{cm}^{-2}$ and $N_d = 1\text{E} + 19\text{cm}^{-2}$ is $-3.82 \times 10^{-1} eV$, $-5.02 \times 10^{-1} eV\ and\ -5.16 \times 10^{-1} eV$ respectively. This is because the potential barrier is very high at low temperature and the increases in the doping concentration increase the height of the barrier potential as such the electrons required a high potential from the source to the drain along the channel. This conforms with a reported by Rahman et al. in 2003 and Gana et al in 2021 that the device exhibits a strong drain electron injection and the MOSFET is under the on-state condition because a high drain bias lowers the energy in the drain and a high gate voltage lower the potential energy barrier, which allowed electrons to flow from source to drain [28, 29]. The energy barrier between the drain and the source along the channel at low gate voltage is high this makes the device to be in the off state. The velocity of the electrons increases along the channel as the temperature increases to an average temperature (350K) as shown in Figures 20, 21 and 22, and the energy of the electron along the channel in the sub-band is lowed with high electron density as described in Figures 7. As the channel length increases the gate voltage also increases from $V_{GS} = 0.5v$ to $V_{GS} = 1.5v$ this causes the energy to also increase with increases in the doping concentration to overcome the barrier potential and the device is in the on-current state (I_{on}). This is in agreement with a report by Ali et al in 2015 that the variation of on-state current decreases as channel doping concentration is increased [30]. There is a barrier near the source end of the channel and the increase in the doping concentration at high temperature $(650\ and\ 850k)$ as shown in Figures 11 and 12 increases the potential energy profile which causes a significant decrease in the electron density. This decrease in electron density allowed the electrons to have such high energy to cross through the channel easier from the source to the drain. When the doping concentration is greater than or equal to $N_d = 1\text{E} + 16\ \text{cm}^{-2}$ the energy is almost constant as the channel increases above 10nm at all temperatures. This shows that increases in the doping level of concentration increase the potential profile thereby decreasing the leakage current and increases in the threshold voltage

V. Conclusion

In this work, the influence of body doping concentration on the quasi-ballistic electron transport in a DG-MOSFET is investigated to analyze the electronic characteristics such as the average electron velocity, drain current, electron density, sub-band energy profile under 50K, 350K, and 850K of temperatures using NanoMOS version 4.0.4 simulation software. It was observed that when the doping concentration is above $\text{N}_\text{d} = 1\text{E} + 18\text{cm}^{-2}$ the average electron velocity is relatively constant as the channel length increases above 14nm and the drain current is almost constant, with slightly constant resistance from the source to the drain throughout the channel. The lower doping concentration of $N_d = 1\text{E} + 04\ \text{cm}^{-2}$, $N_d = 1\text{E} + 08\text{cm}^{-2}$ and $N_d = 1\text{E} + 12\text{cm}^{-2}$ showed an identical output characteristic with higher average electron velocity at all temperatures and the electron density and when the doping concentration is $N_d = 1\text{E} + 16\text{cm}^{-2}$ it is slightly higher because the potential barrier is very high at low temperature and the increases in the doping concentration increase the height of the barrier potential as such the electrons required a high potential from the source to the drain along the channel. It was observed that a change in the gate voltage makes the electron inversion stronger when the doping concentration increases resulting in a stronger On-State current because threshold voltage is more sensitive to doping concentration greater than $\text{N}_\text{d} = 1\text{E} + 18\text{cm}^{-2}$ and also more sensitive to the mobility of the electron at high temperatures. Also, the body doping concentration increase the height of the barrier potential (electron density decrease) at all temperatures and the number of electron entering the channel decreases, this causes a decrease in the On-State current. This shows that increases in the doping level of concentration increase the potential profile thereby decreasing the leakage current and increases in the threshold voltage.

Reference

[1] C. Y. Ooi and S. K. King, "Temperature Variation Effects In Nano-Mosfets Based on Simulation Study," *International Journal of Education and Research,* vol. 1, no. 2, pp. 1-17, 2013.

[2] O. C. Yee and S. K. Lim, "Simulation Study On The Electrical Performance Of Equilibrium Thin-Body Double-Gate Nano-Mosfet," *Jurnal Teknologi,* vol. 76, no. 1, p. 87–95, 2015.

[3] M. Cheralathan, "Compact modeling for multi-gate MOSFETS using advanced transport models," *PhD thesis, universitat rovira i virgili Department of Electronic, Electric and Automatic Engineering.,* p. 149, 2013.

[4] S. M. Gana, G. S. M. Galadanci, T. H. Darma, A. Tijjani, A. Musa and S. Muhammad, "Investigation Of The Effect of Temperature on the Drain Current of a 10nm Double Gate (DG) MOSFET," *Bayero Journal of Physics and Mathematical Sciences,* vol. 12, no. 1, pp. 103-109, 2021.

[5] A. Anand and S. Sinha, "Performance Evaluation of Logic Gates Based On Carbon Nanotube Field Effect Transistor," *International Journal of Recent Technology and Engineering (IJRTE),* vol. 2, no. 5, pp. 120-125., 2013.

[6] K. S. Mane and P. P. Narwade, "Efficient digital circuits based on CNTFET," *International Journal of Electrical and Electronics Engineers,* vol. 7, no. 1, pp. 467-473, 2015.

[7] K. Y. Vinay and K. R. Ashwani, "Impact of Channel Doping on DG-MOSFET Parameters in Nano Region- TCAD Simulation," *Internation Journal of Computer Applications,* vol. 37, no. 11, pp. 36-41, 2012.

[8] S. Yashu and R. Sanjeev, "Physical Parameter Variation Analysis on the Performance Characteristics of Nano DG-MOSFETs," *Circuits and Systems,* vol. 12, pp. 39-53, 2021.

[9] M. S. Viranjay and S. Ghanshyam, MOSFET Technologies for Double-Pole Four-Throw Radio-Frequency Switch, Switzerland : Springer Science and Business Media LLC, 2014.

[10] Y. Taur, "Analytic solutions of charge and capacitance in symmetric and asymmetric double-gate MOSFETs," *IEEE Transcation on Electron Device,* vol. 48, no. 12, pp. 2861-2869, 2001.

[11] M. Ieong, H. S. P. Wong, E. Nowak, J. Kedzierski and E. C. Jones, "High performance double-gate device technology challenges and opportunities," in *Proceedings International Symposium on Quality Electronic Design*, San Jose, CA, USA, 2002.

[12] L. Huaxin, L. Wei-Yuan and T. Yuan, "Effect of body doping on double-gate MOSFET characteristics," *Semiconductor Science and Technology (IOP Publishing),* vol. 23, no. 1, pp. 1-6, 2008.

[13] J. K. Schaeffer, C. Capasso, L. R. C. Fonseca, S. Samavedam, D. C. Gilmer and Y. Liang, "Challenges for the integration of metal gate electrodes," *International Electron Devices Meeting (IEDM),* pp. 287-290, 2004.

[14] Kavalieros, et al., "Tri-Gate Transistor Architecture with High-k Gate Dielectrics, Metal Gates and Strain Engineering," in *Symposium on VLSI Technology, Digest of Technical Papers*, Honolulu, HI, USA, 2006.

[15] D. Dey, D. De, A. Ahmadian, G. Ferial and S. Norazak, "Electrically Doped Nanoscale Devices Using First-Principle Approach: A Comprehensive Survey.," *Nanoscale Reserch Letter,* vol. 20, pp. 16-20, 2021.

[16] Jeon, I. S. et al., "A novel methodology on tuning work function of metal gate using stacking bi-metal layers," *IEDM Technical Digest. IEEE International Electron Devices Meeting,* pp. 302-306, 2004.

[17] S. Joseph, G. James and T. V. Mathew, "Effect of channel layer doping on the performance of nanoscale DG MOSFETs," in *International Conference on Emerging Trends in Electronic and Photonic Devices & Systems*, Varanasi, India, 2009.

[18] A. A. Ziabari, M. Charmi and H. R. Mashayekhi, "The Impact of body doping concentration in the performance of Nano MOSFET: A Quantum Simulation," *Chinese Jounal of Physics,* vol. 51, no. 4, pp. 844-853, 2013.

[19] Z. Ren, S. Goasguen, A. Matsudaira, S. S. Ahmed, K. Cantley, Y. Liu, Y. Gao, X. Wang and M. Lundstrom, "NanoMOS," 22 March 2006. [Online]. Available: https://nanohub.org/resources/nanomos.

[20] Wang, "NanoMOS 4.0: A Tool To Explore Ultimate Si Transistors and Beyond," Purdue University, West Lafayette, Indiana, 2010.

[21] K. Natori, "Ballistic metal–oxide–semiconductor field effect transistor," *Jounal of Applied Physics*, vol. 76 , no. 8, p. 4879–4890, 1994.

[22] C. Jeong, D. Antoniadis and M. Lundstrom, "On Backscattering and Mobility in Nanoscale Silicon MOSFETs," *Birck and NCN Publications*, vol. 59, no. 11, pp. 2762-2769, 2009.

[23] M. Lundstrom and Z. Ren, "Essential Physics of Carrier Transport in Nanoscale MOSFETs," *IEEE Transaction Electron Devices*, vol. 49, no. 1, pp. 133-141, 2002.

[24] D. K. Shroder, Semiconductor Material and Device Characterization, 2 ed., New York: Wiley, 1998, p. 790.

[25] C. Y. Ooi and S. K. Lim, "Study of Timing Characteristics of NOT Gate Transistor Level Circuit Implemented Using Nano-MOSFET by Analyzing Sub-Band Potential Energy Profile and Current-Voltage Characteristic of Quasi-Ballistic Transport," *World Journal of Nano Science and Engineering*, *6*, pp. 177-188, 2016.

[26] A. A. Ahmadain, K. P. Roenker and K. A. Tomko, "A Study of the Performance of Ballistic Nanoscale MOSFETS Using Classical and Quantum Ballistic Transport Models," *Sixth IEEE Conference on Nanotechnology, Cincinnati, OH, USA*, vol. 3, no. 6, pp. 16-19, 2006.

[27] Z. Ren, R. Venugopal, S. Goasguen, S. Datta and M. S. Lundstrom, "nanoMOS 2.5: A Two-Dimensional Simulator for Quantum Transport in Double-Gate MOSFETs," *IEEE Transaction on Electron Devices*, vol. 50, no. 9, pp. 1914-1925, 2003.

[28] A. Rahman, J. Guo, S. Datta and M. S. Lundstrom, "Theory of Ballistic Nanotransistors," *IEEE Transactions on Electron Devices*, vol. 50, no. 9, pp. 1853-1864, 2003.

[29] S. M. Gana, G. S. M. Galadanci, T. H. Darma and A. Tijjani, "Effect of Temperature on The Quasi Ballistic Transport of A Double Gate Nano-Mosfet," *NIPES Journal of Science and Technology Research*, vol. 3, no. 2, pp. 1-10, 2021.

[30] N. Ali, D. Dheer, S. Paliwal and C. Periasamy, "TCAD analysis of variation in channel doping concentration on 45nm Double-Gate MOSFET parameters," in *Annual IEEE India Conference (INDICON)*, New Delhi, India, 2015.